# Optical Diode Effect at Spin-Wave Excitations of the Room-Temperature Multiferroic BiFeO₃

I. Kézsmárki,[1] U. Nagel,[2] S. Bordács,[1] R. S. Fishman,[3] J. H. Lee,[3] Hee Taek Yi,[4] S.-W. Cheong,[4] and T. Rõõm[2]

[1]*Department of Physics, Budapest University of Technology and Economics and MTA-BME Lendület Magneto-optical Spectroscopy Research Group, 1111 Budapest, Hungary*
[2]*National Institute of Chemical Physics and Biophysics, 12618 Tallinn, Estonia*
[3]*Materials Science and Technology Division, Oak Ridge National Laboratory, Oak Ridge, Tennessee 37831, USA*
[4]*Rutgers Center for Emergent Materials and Department of Physics and Astronomy, Rutgers University, Piscataway, New Jersey 08854, USA*
(Received 20 May 2015; published 15 September 2015)

Multiferroics permit the magnetic control of the electric polarization and the electric control of the magnetization. These static magnetoelectric (ME) effects are of enormous interest: The ability to read and write a magnetic state current-free by an electric voltage would provide a huge technological advantage. Dynamic or optical ME effects are equally interesting, because they give rise to unidirectional light propagation as recently observed in low-temperature multiferroics. This phenomenon, if realized at room temperature, would allow the development of optical diodes which transmit unpolarized light in one, but not in the opposite, direction. Here, we report strong unidirectional transmission in the room-temperature multiferroic BiFeO₃ over the gigahertz-terahertz frequency range. The supporting theory attributes the observed unidirectional transmission to the spin-current-driven dynamic ME effect. These findings are an important step toward the realization of optical diodes, supplemented by the ability to switch the transmission direction with a magnetic or electric field.

BiFeO₃ is by far the most studied compound in the populous family of multiferroic and magnetoelectric (ME) materials [1–9]. While experimental studies have already reported about the first realizations of the ME memory function using BiFeO₃-based devices [6–9], the origin of the ME effect is still under debate due to the complexity of the material. Because of the low symmetry of iron sites and iron-iron bonds, the magnetic ordering can induce local polarization via each of the three canonical terms [10]—the spin-current, exchange-striction, and single-ion mechanisms. While the spin-current term has been identified as the leading contribution to the magnetically induced ferroelectric polarization in various studies [5,11,12], the spin-driven atomic displacements [13] and the electrically induced shift of the spin-wave (magnon) resonances [14] were interpreted based on the exchange-striction and single-ion mechanisms, respectively.

In the magnetically ordered phase below $T_N = 640$ K, BiFeO₃ possesses an exceptionally large spin-driven polarization [13], if not the largest among all known multiferroic materials. Nevertheless, its systematic study has long been hindered by the huge lattice ferroelectric polarization ($\mathbf{P}_0$) developing along one of the cubic $\langle 111 \rangle$ directions at $T_C = 1100$ K and by the lack of single-domain ferroelectric crystals. Owing to the coupling between $\mathbf{P}_0$ and the spin-driven polarization, in zero magnetic field they both point along the same [111] axis. A recent systematic study of the static ME effect revealed additional spin-driven polarization orthogonal to the [111] axis [12].

The optical ME effect of the magnon modes in multiferroics, which gives rise to the unidirectional transmission in the gigahertz-terahertz frequency range, has recently become a hot topic in materials science [15–24]. The difference in the absorption coefficients ($\alpha$) of beams counterpropagating in such ME media—called the nonreciprocal directional dichroism (NDD)—can be expressed for linear light polarization as [15,16]

$$\Delta\alpha_k(\omega) = \alpha_{+k}(\omega) - \alpha_{-k}(\omega) \approx \frac{2\omega}{c}\text{Im}\{\chi_{\gamma\delta}^{me}(\omega) + \chi_{\delta\gamma}^{em}(\omega)\}. \tag{1}$$

The dynamic ME susceptibility tensors $\hat{\chi}^{me}(\omega)$ and $\hat{\chi}^{em}(\omega)$, respectively, describe the magnetization generated by the oscillating electric field of light, $\Delta M_\gamma^\omega = (\varepsilon_0/\mu_0)^{1/2}\chi_{\gamma\delta}^{me}(\omega)E_\delta^\omega$, and the electric polarization induced by its oscillating magnetic field, $\Delta P_\delta^\omega = (\varepsilon_0\mu_0)^{1/2}\chi_{\delta\gamma}^{em}(\omega)H_\gamma^\omega$. Here $\varepsilon_0$ and $\mu_0$ are the vacuum permittivity and permeability, respectively, while $\gamma$ and $\delta$ stand for the Cartesian coordinates. Since the two cross-coupling tensors are connected by the time-reversal operation $[\ldots]'$ according to $[\chi_{\gamma\delta}^{me}(\omega)]' = -\chi_{\delta\gamma}^{em}(\omega)$, the NDD becomes $\Delta\alpha_k(\omega) = (2\omega/c)\text{Im}\{\chi_{\gamma\delta}^{me}(\omega) - [\chi_{\gamma\delta}^{me}(\omega)]'\}$. In other words, the NDD emerges for simultaneously electric- and magnetic-dipole active excitations, and its magnitude is

determined by the time-reversal odd parts of the off-diagonal $\chi_{\gamma\delta}^{me}(\omega)$ tensor elements [16–19]. The schematic representation of the optical diode function in ME media is shown in Fig. 1. In this Letter, we demonstrate this functionality to emerge at spin-wave excitations of $BiFeO_3$ located in the gigahertz-terahertz spectral range.

Extensive studies on various low-temperature multiferroic compounds have confirmed that unidirectional transmission is a general inherent property of this class of materials [15–24], and the symmetry requirements for this phenomenon have been classified [25]. Moreover, it has been pointed out that the static ME effect of multiferroics is mainly governed by the NDD of their magnon excitations [26].

In the cycloidal spin state of $BiFeO_3$ [27], several low-frequency collective modes have been observed by light absorption [28–30] and Raman spectroscopy [7,14,31]. Though the electric-field-induced shift of the resonance frequencies observed in the Raman study indicates the ME nature of these magnon modes [14], the optical ME effect

has not been investigated in $BiFeO_3$. Here, we performed absorption measurements in the gigahertz-terahertz spectral range on single-domain ferroelectric $BiFeO_3$ crystals [32] with $\mathbf{P}_0\|[111]$ between $T = 4$ and 300 K in magnetic fields up to $\mu_0 H = 17$ T [33]. We found that some of the magnon modes exhibit strong NDD. We identified the minimal set of spin-driven polarization terms and quantitatively reproduced both the spectral shape and the field dependence of the NDD solely by the spin-current mechanism.

The experimental configurations are schematically illustrated in Fig. 2. Absorption spectra were obtained for light beams propagating along [001] with two orthogonal linear polarizations, $\mathbf{E}^\omega\|[1\bar{1}0]$ and $\mathbf{E}^\omega\|[110]$. Static magnetic fields ($\pm H$) were applied perpendicular to the light propagation direction along either [110] or [1$\bar{1}$0].

In simple magnets, such as ferromagnets, the sign change of the magnetization corresponds to the time-reversal operation. Thus, it is equivalent to the reversal of the light propagation direction. Owing to experimental limitations, in such cases, the absorption change upon the magnetic-field-induced reversal of the magnetization, $\Delta\alpha_H = \alpha_{+H,+k} - \alpha_{-H,+k}$, is typically detected instead of
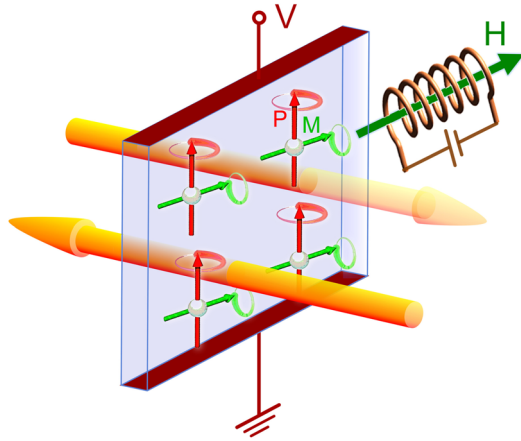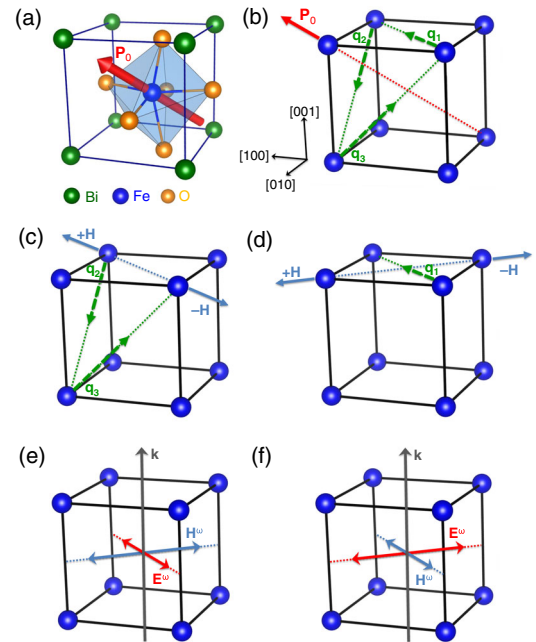


FIG. 1 (color online). Ferro-type ordering of the local electric dipoles (red arrows) and magnetic moments (green arrows) produces a ferroelectric polarization $P$ and a spontaneous magnetization $M$, respectively. Light interacts with both ferroic order parameters; hence, upon illumination $P$ and $M$ oscillate coherently with the electromagnetic field around their equilibria. The polarization dynamics is governed by both the usual dielectric permittivity and the optical ME effect $\chi^{em}(\omega)$. While the dielectric response is independent of the light propagation direction, the polarization induced via the optical ME effect has opposite sign for counterpropagating light beams; hence, the two terms can interfere either constructively or destructively. Similarly, the magnetization dynamics is governed by the interference between the magnetization induced via the magnetic permeability and the optical ME effect $\chi^{me}(\omega)$. Consequently, the transmitted intensity depends on the propagation direction (intense and pale yellow beams) even for unpolarized light and can be exploited to produce optical diodes transmitting light in one, but not in the opposite, direction. The transmitting direction can be reversed by switching the sign of either $P$ via an electric voltage ($V$) or $M$ by an external magnetic field ($H$).



FIG. 2 (color online). (a) Pseudocubic unit cell of $BiFeO_3$ showing the positions of Bi, Fe, and O ions. The lattice ferroelectric polarization $\mathbf{P}_0\|[111]$ is schematically indicated on the Fe site. (b) Illustration of the three equivalent directions of the cycloidal ordering vector $\mathbf{q}_i$ on the Fe sublattice. The frame of reference is common to all panels. (c) In magnetic fields ($\pm H$) applied along [1$\bar{1}$0], cycloidal domains with $\mathbf{q}_2$ and $\mathbf{q}_3$ are equally favored, while the domain with $\mathbf{q}_1$ is suppressed [37,38]. (d) In magnetic fields ($\pm H$) applied along [110], only the cycloidal domain with $\mathbf{q}_1$ is stable [37,38]. (e),(f) The propagation direction ($\mathbf{k}$) and the two orthogonal polarizations of light beams traveling in the material.

the absorption change associated with the reversal of the light propagation direction, $\Delta\alpha_k = \alpha_{+H,+k} - \alpha_{+H,-k}$. Though the relation $\Delta\alpha_k = \Delta\alpha_H$ does not necessarily hold for complex spin structures, such as BiFeO₃, $\Delta\alpha_k$ and $\Delta\alpha_H$ spectra obtained from our calculations are equal within the numerical precision for the experimental configurations studied here.

Figure 3 shows the absorption spectra measured in four different configurations, i.e., for two orientations of the magnetic field and two light polarizations. The absorption coefficient at several magnon resonances depends on the sign of the magnetic field. This difference is stronger for $\mathbf{H}\|[1\bar{1}0]$ and most pronounced for the lowest-frequency mode $\Psi_0$ in Fig. 3(a) when $\mathbf{H}\|[1\bar{1}0]$ and $\mathbf{E}^\omega\|[110]$. With increasing magnetic field, this resonance becomes almost transparent for $+H$, while its absorption increases for $-H$. For this mode, the relative absorption difference $\Delta\alpha_H/\bar{\alpha}_H \approx 1$, where $\bar{\alpha}_H = \alpha_{+H,+k} + \alpha_{-H,+k}$ is the mean absorption. We also measured the absorption spectra with both light polarizations for $\mathbf{H}\|\mathbf{k}\|[001]$ and could not detect any difference between $\pm H$.

To reproduce the observed NDD on a microscopic basis, we adopt the spin model of Refs. [37,38], which successfully describes the magnetic-field dependence of the magnon resonances [33]. Similarly to the static ME effect, all three basic mechanisms—the spin-current, exchange-striction, and single-ion mechanisms—can, in principle, contribute to the optical ME effect. By including all symmetry-allowed spin-driven polarization terms, we calculated the optical ME susceptibilities $\hat{\chi}^{me}(\omega)$ and $\hat{\chi}^{em}(\omega)$, the dielectric permittivity $\hat{\varepsilon}(\omega)$, and the magnetic permeability $\hat{\mu}(\omega)$ [15,16]. Next, we numerically solved the Maxwell equations by including these response functions in the constitutive relations and calculated the transmission of linearly polarized incoming beams for both backward and forward propagation. The same calculation done for both field directions, $\pm H$, confirmed that $\Delta\alpha_k = \Delta\alpha_H$.

To identify the spin-driven polarization terms contributing to the optical ME effect, we performed a systematic fitting of the measured $\Delta\alpha_H(\omega)$ by treating the magnitude of the different terms as free parameters. We found that the NDD spectra are closely reproduced by the following two types of spin-current terms:

$$P_\alpha^{SC} = \frac{1}{N}\sum_{\langle i,j\rangle}\{\lambda_\alpha^{(1)}[\mathbf{e}_{i,j}\times(\mathbf{S}_i\times\mathbf{S}_j)]_\alpha$$
$$+ (-1)^{n_i}\lambda_\alpha^{(2)}[\mathbf{S}_i\times\mathbf{S}_j]_\alpha\}, \qquad (2)$$
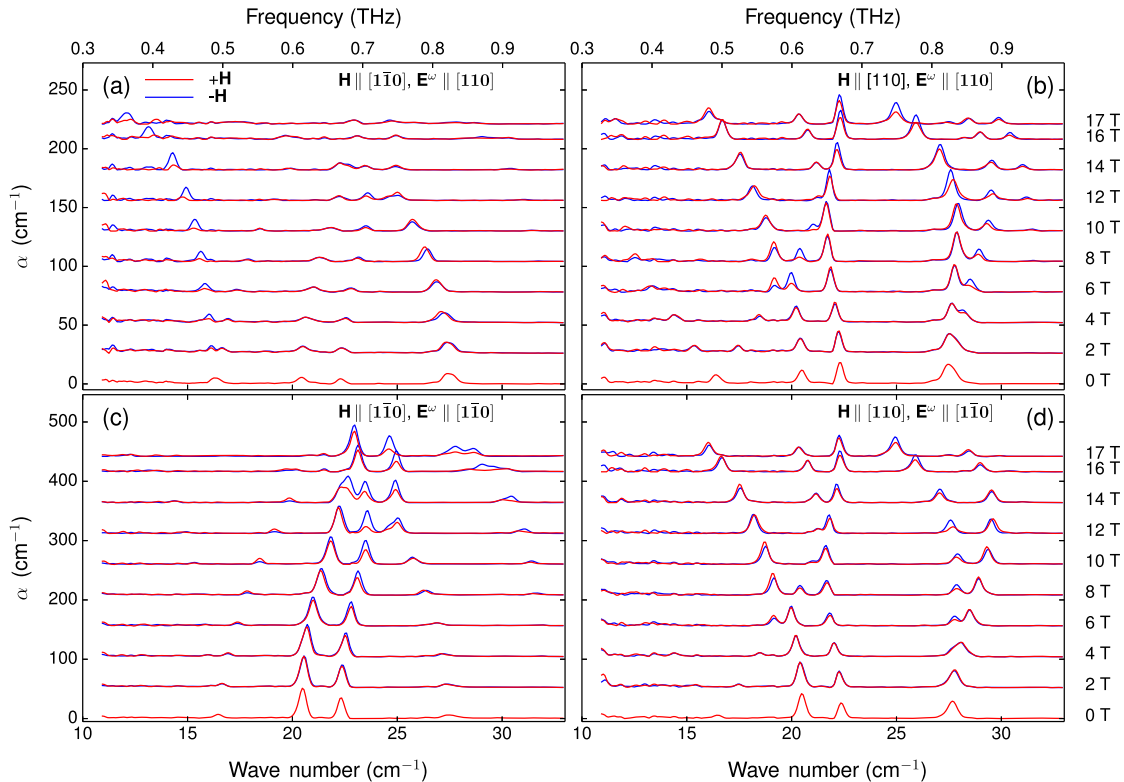


FIG. 3 (color online).   (a)–(d) Magnetic-field-dependent part of the absorption spectra measured at $T = 2.5$ K for the two orientations of the magnetic field (**H**) and the two orthogonal polarizations (**E**$^\omega$) schematically shown in Fig. 2. The light propagation direction is common to all configurations, $\mathbf{k}\|[001]$. Absorption spectra measured in different magnetic fields are shifted vertically in proportion to the magnitude of the field, and spectra recorded in $+H$ and $-H$ are plotted with red and blue lines, respectively. Spectra shown in (a) and (c) represent absorption from the $\mathbf{q}_1$ cycloidal domain, while spectra in (b) and (d) have contributions from $\mathbf{q}_2$ and $\mathbf{q}_3$ domains.

where the summation goes over neighboring spins connected by unit vectors $\mathbf{e}_{i,j}$ and the integer $n_i$ labels the hexagonal layers along [111]. The dynamic ME effect generated by the spin-current terms is described by the coupling constants $\lambda_\alpha^{(1)}$ and $\lambda_\alpha^{(2)}$, where $\alpha = x', y', z'$ stands for the three coordinates along the axes $\mathbf{x}' \| \mathbf{q}_i$, $\mathbf{y}' \| (\mathbf{P}_0 \times \mathbf{q}_i)$ and $\mathbf{z}' \| \mathbf{P}_0$ [see Fig. 2(b)].

Figure 4 shows the comparison between the measured and calculated NDD spectra for $\mathbf{H} \| [1\bar{1}0]$ with the two orthogonal light polarizations, $\mathbf{E}^\omega \| [1\bar{1}0]$ and $\mathbf{E}^\omega \| [110]$. The best fit was obtained with three independent parameters: $\lambda_{x'}^{(1)} = 0$, $\lambda_{y'}^{(1)} = -2\lambda_{z'}^{(1)} \approx 57.0 \pm 3.1$ nC/cm$^2$, $\lambda_{x'}^{(2)} = \lambda_{z'}^{(2)} \approx 34.5 \pm 2.4$ nC/cm$^2$, and $\lambda_{y'}^{(2)} \approx 11.8 \pm 2.9$ nC/cm$^2$. The population of the two cycloidal domains with $\mathbf{q}_2$ and $\mathbf{q}_3$ propagation vectors was kept equal [37,38]. We note that this limited set of parameters provides only a semiquantitative description of the mean absorption spectra.

We found that additional terms did not further improve the quality of the fit. Hence, the optical ME effect in BiFeO$_3$ is dominated by two types of spin-current polarizations, while the exchange-striction and single-ion polarization terms do not significantly contribute to it. This stems from the general nature of the spin dynamics in BiFeO$_3$. Because of the very weak on-site anisotropy acting on the

$S = 5/2$ iron spins, each magnon mode corresponds to pure precessions of the spins, where the oscillating component of the spin on site $i$, $\delta\mathbf{S}_i^\omega$, is perpendicular to its equilibrium direction $\mathbf{S}_i^0$. This is in contrast to the spin stretching or Higgs modes observed in highly anisotropic magnets [19,39–42]. Since neighboring spins are nearly collinear in the cycloidal state with 62 nm pitch [27], a dynamic polarization is efficiently induced via spin-current terms such as $\delta\mathbf{P}_i^\omega \propto \mathbf{S}_i^0 \times \delta\mathbf{S}_{i+1}^\omega$. In contrast, the dynamic polarization generated by exchange-striction terms such as $\delta\mathbf{P}_i^\omega \propto \mathbf{S}_i^0 \cdot \delta\mathbf{S}_{i+1}^\omega$ is nearly zero.

For $\mathbf{k} \| [001]$, we predict zero NDD when $\mathbf{H} \| [\eta\eta\kappa]$. While this is in agreement with $\Delta\alpha_H = 0$ found for $\mathbf{H} \| [001]$, it cannot account for the finite NDD discerned in Figs. 3(b) and 3(d) for $\mathbf{H} \| [110]$. This discrepancy may come from additional anisotropy terms, neglected in the microscopic spin Hamiltonian adopted from Refs. [37,38], which further reduce the symmetry of the magnetic state.

The temperature dependence of NDD is presented in Fig. 5 for $\mathbf{H} \| \mathbf{E}^\omega \| [1\bar{1}0]$. With increasing temperature, the magnon modes soften [29], and both the mean absorption and the NDD are reduced. Nevertheless, the modes $\Psi_1^{(1)}$ and $\Phi_2^{(1,2)}$ still exhibit considerable NDD, $\Delta\alpha_H \approx 5$ cm$^{-1}$ at room temperature.

Here we studied the unidirectional transmission in the spin excitation spectrum of BiFeO$_3$, the unique multiferroic compound offering a real potential for room-temperature applications up to date. We found that the optical ME effect in BiFeO$_3$ is robust enough to generate considerable NDD in the gigahertz-terahertz range even at room temperature. Our calculations predict a similarly strong optical ME effect for light beams propagating along [111] and [1$\bar{1}$0] whenever $\mathbf{H} \perp \mathbf{k}$. When extending the present work to BiFeO$_3$ films, this provides a freedom to use films with different orientations. Based on the current progress achieved in the electric control of the magnetization in
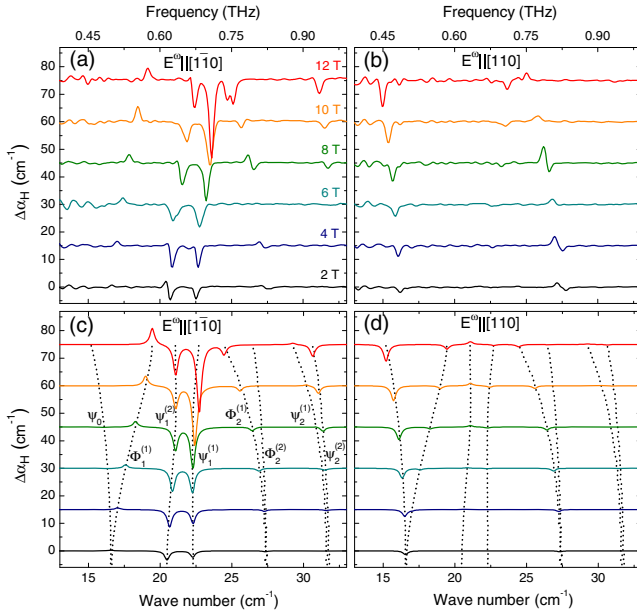


FIG. 4 (color online).   (a),(b) Magnetic-field dependence of the NDD spectra measured at $T = 2.5$ K with the two orthogonal polarizations $\mathbf{E}^\omega \| [1\bar{1}0]$ and $\mathbf{E}^\omega \| [110]$, respectively. Spectra obtained in different magnetic fields along [1$\bar{1}$0] are shifted vertically in proportion to the magnitude of the field. The field values (common to each panel) are indicated on the top of the spectra in (a). (c),(d) NDD spectra predicted by our model for the case of (a) and (b), respectively. The calculated mode frequencies are indicated by dashed lines. For the assignment of the different modes, see Refs. [37,38].
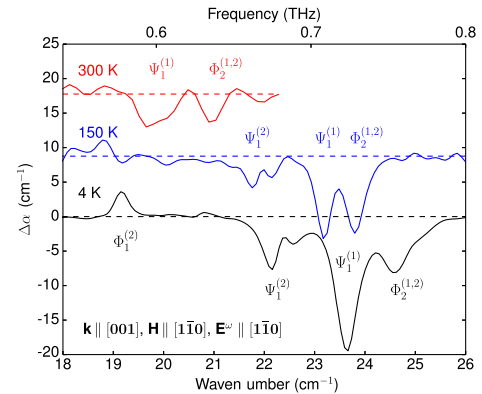


FIG. 5 (color online).   NDD spectra measured in $\mu_0 H = \pm 12$ T at $T = 4$, 150, and 300 K. The magnetic field was applied along [1$\bar{1}$0] and $\mathbf{E}^\omega \| [1\bar{1}0]$. Modes $\Psi_1^{(1)}$ and $\Phi_2^{(1,2)}$ soften and get weaker with increasing temperature but are still clearly observable even at 300 K.

[1] T. Kimura, T. Goto, H. Shintani, K. Ishizaka, T. Arima, and Y. Tokura, Nature (London) **426**, 55 (2003).
[2] M. Fiebig, J. Phys. D **38**, R123 (2005).
[3] N. A. Spaldin and M. Fiebig, Science **309**, 391 (2005).
[4] W. Eerenstein, N. D. Mathur, and J. F. Scott, Nature (London) **442**, 759 (2006).
[5] S.-W. Cheong and M. Mostovoy, Nat. Mater. **6**, 13 (2007).
[6] L. W. Martin, Y.-H. Chu, and R. Ramesh, Mater. Sci. Eng. R **68**, 89 (2010).
[7] D. Sando et al., Nat. Mater. **12**, 641 (2013).
[8] J. T. Henron, J. L. Bosse, Q. He, Y. Gao, M. Trassin, L. Ye, J. D. Clarkson, C. Wang, J. Liu, S. Salahuddin, D. C. Ralph, D. G. Schlom, J. Iniguez, B. D. Huey, and R. Ramesh, Nature (London) **516**, 370 (2014).
[9] F. Matsukura, Y. Tokura, and H. Ohno, Nat. Nanotechnol. **10**, 209 (2015).
[10] C. Jia, S. Onoda, N. Nagaosa, and J. H. Han, Phys. Rev. B **76**, 144424 (2007).
[11] H. Katsura, N. Nagaosa, and A. V. Balatsky, Phys. Rev. Lett. **95**, 057205 (2005).
[12] M. Tokunaga, M. Akaki, T. Ito, S. Miyahara, A. Miyake, H. Kuwahara, and N. Furukawa, Nat. Commun. **6**, 5878 (2015).
[13] S. Lee, M. T. Fernandez-Diaz, H. Kimura, Y. Noda, D. T. Adroja, Seongsu Lee, J. Park, V. Kiryukhin, S.-W. Cheong, M. Mostovoy, and J.-G. Park, Phys. Rev. B **88**, 060103(R) (2013).
[14] P. Rovillain, R. de Sousa, Y. Gallais, A. Sacuto, M. A. Masson, D. Colson, A. Forget, M. Bibes, A. Barthelemy, and M. Cazayous, Nat. Mater. **9**, 975 (2010).
[15] I. Kezsmarki, D. Szaller, S. Bordacs, V. Kocsis, Y. Tokunaga, Y. Taguchi, H. Murakawa, Y. Tokura, H. Engelkamp, T. Room, and U. Nagel, Nat. Commun. **5**, 3203 (2014).
[16] S. Miyahara and N. Furukawa, J. Phys. Soc. Jpn. **81**, 023712 (2012).
[17] I. Kezsmarki, N. Kida, H. Murakawa, S. Bordacs, Y. Onose, and Y. Tokura, Phys. Rev. Lett. **106**, 057403 (2011).
[18] S. Bordacs, I. Kezsmarki, D. Szaller, L. Demko, N. Kida, H. Murakawa, Y. Onose, R. Shimano, T. Room, U. Nagel, S. Miyahara, N. Furukawa, and Y. Tokura, Nat. Phys. **8**, 734 (2012).
[19] S. Miyahara and N. Furukawa, J. Phys. Soc. Jpn. **80**, 073708 (2011).
[20] M. Saito, K. Ishikawa, K. Taniguchi, and T. Arima, Phys. Rev. Lett. **101**, 117402 (2008).
[21] M. Saito, K. Taniguchi, and T. Arima, J. Phys. Soc. Jpn. **77**, 013705 (2008).
[22] M. Saito, K. Ishikawa, S. Konno, K. Taniguchi, and T. Arima, Nat. Mater. **8**, 634 (2009).
[23] Y. Takahashi, R. Shimano, Y. Kaneko, H. Murakawa, and Y. Tokura, Nat. Phys. **8**, 121 (2012).
[24] Y. Takahashi, Y. Yamasaki, and Y. Tokura, Phys. Rev. Lett. **111**, 037204 (2013).
[25] D. Szaller, S. Bordacs, and I. Kezsmarki, Phys. Rev. B **87**, 014421 (2013).
[26] D. Szaller, S. Bordacs, V. Kocsis, T. Room, U. Nagel, and I. Kezsmarki, Phys. Rev. B **89**, 184419 (2014).
[27] I. Sosnowska, T. Peterlin-Neumaier, and E. Steichle, J. Phys. C **15**, 4835 (1982).
[28] U. Nagel, R. S. Fishman, T. Katuwal, H. Engelkamp, D. Talbayev, H. T. Yi, S.-W. Cheong, and T. Room, Phys. Rev. Lett. **110**, 257201 (2013).
[29] D. Talbayev, S. A. Trugman, S. Lee, H. T. Yi, S.-W. Cheong, and A. J. Taylor, Phys. Rev. B **83**, 094403 (2011).
[30] S. Skiadopoulou, V. Goian, C. Kadlec, F. Kadlec, X. F. Bai, I. C. Infante, B. Dkhil, C. Adamo, D. G. Schlom, and S. Kamba, Phys. Rev. B **91**, 174108 (2015).
[31] M. Cazayous, Y. Gallais, A. Sacuto, R. de Sousa, D. Lebeugle, and D. Colson, Phys. Rev. Lett. **101**, 037601 (2008).
[32] D. Talbayev, S. Lee, S.-W. Cheong, and A. J. Taylor, Appl. Phys. Lett. **93**, 212906 (2008).
[33] See Supplemental Material at http://link.aps.org/supplemental/10.1103/PhysRevLett.115.127203 for details of the experimental method, the microscopic spin model, and Refs. [34–36].
[34] A. P. Pyatakov and A. K. Zvezdin, Eur. Phys. J. B **71**, 419 (2009).
[35] C. Ederer and N. A. Spaldin, Phys. Rev. B **71**, 060401(R) (2005).
[36] M. Matsuda, R. S. Fishman, T. Hong, C. H. Lee, T. Ushiyama, Y. Yanagisawa, Y. Tomioka, and T. Ito, Phys. Rev. Lett. **109**, 067205 (2012).
[37] R. S. Fishman, J. T. Haraldsen, N. Furukawa, and S. Miyahara, Phys. Rev. B **87**, 134416 (2013).
[38] R. S. Fishman, Phys. Rev. B **87**, 224419 (2013).
[39] K. Penc, J. Romhanyi, T. Room, U. Nagel, A. Antal, T. Feher, A. Janossy, H. Engelkamp, H. Murakawa, Y. Tokura, D. Szaller, S. Bordacs, and I. Kezsmarki, Phys. Rev. Lett. **108**, 257203 (2012).
[40] M. Matsumoto, M. Soda, and T. Masuda, J. Phys. Soc. Jpn. **82**, 093703 (2013).
[41] M. Matsumoto, J. Phys. Conf. Ser. **592**, 012123 (2015).
[42] M. Matsumoto, J. Phys. Soc. Jpn. **84**, 034701 (2015).